Chapter 8
An Ultra-low Power, Robust Photoplethysmographic Readout Exploiting Compressive Sampling, Artifact Reduction, and Sensor Fusion

Venkata Rajesh Pamula, Chris Van Hoof, and Marian Verhelst

8.1 Introduction

There is an ever-increasing interest in wearable medical devices as a reaction to the population's increased vulnerability to cardiovascular diseases (CVD) and mental disorders. Continuous monitoring of heart rate (HR) and heart rate variability (HRV) provide critical information about an individual's cardiovascular and mental health state [1]. Electrocardiography (ECG) is one of the standard signal acquisition modalities to continuously monitor HR and HRV. Despite being a popular technique, continuous monitoring of HR through ECG reduces patient comfort, particularly for long-term monitoring, due to the usage of electrodes and its requirements regarding skin preparation.

Photoplethysmography (PPG)-based continuous HR and HRV monitoring is emerging as an attractive alternative to ECG-based methods. Unlike ECG, PPG is a non-contact, single-point biosignal measurement technique, resulting in an increased patient comfort. PPG acquisition involves shining light (usually at 660 nm and/or 900–940 nm wavelengths, corresponding to red (R) and infrared (IR), respectively), through tissue and detecting the transmitted/reflected component of the light [2]. Light-emitting diodes (LEDs) are commonly used as light source, while the transmitted/reflected component is measured using photodiodes (PDs). Although PPG-based HR measurement is a well-understood concept, its usage in continuous monitoring is hindered due to its very large power consumption compared to ECG-

V.R. Pamula (✉) • C. Van Hoof
ESAT, KU Leuven and IMEC, Leuven, Belgium
e-mail: pamula@imec.be

M. Verhelst
ESAT, KU Leuven, Leuven, Belgium

P. Harpe et al. (eds.), *Hybrid ADCs, Smart Sensors for the IoT, and Sub-1V & Advanced Node Analog Circuit Design*, DOI 10.1007/978-3-319-61285-0_8

based methods. The power consumption of a typical PPG acquisition system ranges from few mWs to tens of mWs, dominated by the power consumption of the LED driver. Moreover, PPG acquisition is highly susceptible to motion artifacts, degrading its robustness and reliability.

In this chapter, a compressive sampling (CS)-based PPG readout is presented, which enables reduction of relative LED driver power consumption by up to a factor of 30x. The ASIC also integrates a digital back-end, which performs direct feature extraction from the CS signal to estimate average HR, without requiring complex reconstruction techniques. The possibility of artifact reduction, leveraging on sensor fusion and a spectral subtraction technique, is also presented.

8.2 Overview of Photoplethysmogram (PPG) Acquisition

As indicated in Sect. 8.1, PPG acquisition is an optical-sensing modality, which can be performed both in transmission and reflection modes. Figure 8.1 shows the principle of PPG acquisition, using transmission mode. The photocurrent (I_{ph}) acquired by the PD comprises of a small AC component, which arises due to increased flow of blood during systole. The AC component rides on top of a relatively large DC component, arising due to bone and the static blood in the tissue. Since the AC component is related to heart pulsation, its frequency is highly correlated to the HR. The peak-to-peak value of the AC component of the photocurrent depends on several factors including the intensity of the LED light, the quantum efficiency of the PD, the skin tone of the subject mode of PPG acquisition, and the location at which the acquisition is being performed [3]. In terms of relative values, the AC component is typically 1–4% of the DC component. In a voltage mode signal processing system, this photocurrent is converted into a voltage signal through a transimpedance amplifier (TIA), which is then processed further (Fig. 8.2).

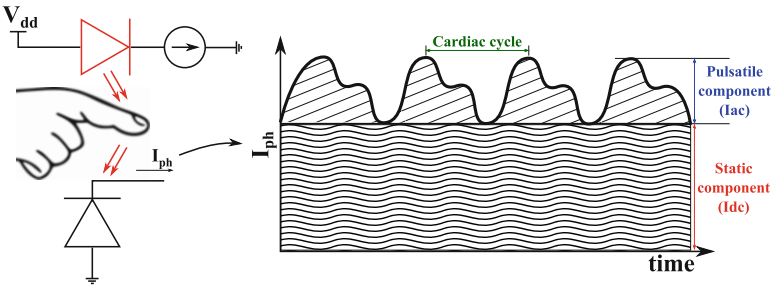

Fig. 8.1 Principle of transmission mode PPG acquisition

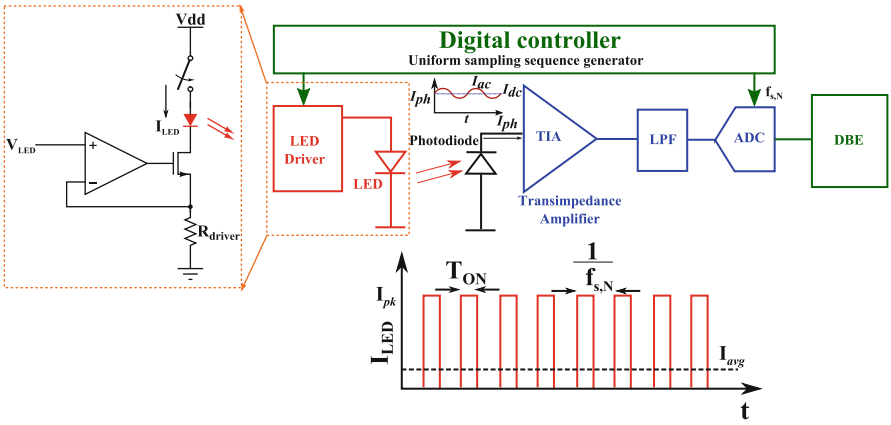

Fig. 8.2 Conventional PPG acquisition system employing uniform LED stimulation and sampling

The relatively small AC component in comparison to the DC component necessitates the need for a low-noise and large dynamic-range (DR) readout. Further, to conserve power in the LED driver, the LED stimulation is typically pulsed, with duty cycles in the range 0.25–2%, implying the need for fast settling of the TIA. The ON duration of the LED and hence the duty cycle (D) of the LED determine the average current (I_{avg}) flowing through the LED (I_{LED}) and hence its power consumption (Fig. 8.2). While the LED driver power can be reduced by further reducing D, it poses stringent requirements on the bandwidth of the TIA, thereby increasing its power consumption. In [4], the authors combined the LED driver power and readout power to formulate an optimization problem to arrive at optimum value for D which minimizes the entire system power. The implemented system is reported to consume 1.5 mW, of which 340 μWs is dissipated in the LED driver. However, [4] does not formulate the power consumption of TIA in terms of noise and assumes it is bandwidth limited. This assumption is not necessarily valid when high SNRs are required at low LED stimulation currents as the noise of the TIA dictates the readout power consumption in such cases rather than its bandwidth.

A highly sensitive analog front-end (AFE) for PPG acquisition using ambient light is proposed in [5]. The proposed AFE employs a wide range logarithmic digital-to-resistance converter (DRC) and a nonuniform quantizer based on laddered inverter quantizer (LIQAF). The AFE, implemented in a 0.18 μm CMOS process, consumes <4 μWs of power from a 0.5 V supply. While the possibility of measuring HR using ambient has been demonstrated with the proposed AFE, its efficacy is highly dependent on the ambient light levels. Moreover, the SNR achieved under nominal lighting conditions is not reported. This, therefore, limits the applicability of the proposed AFE in [5], particularly under low ambient light and low perfusion conditions, which necessitate the use of LED as light source. Therefore, it is desirable to explore techniques that can potentially reduce the relative LED driver

power consumption. Enabling this objective, by employing the principles of CS, to reduce the relative LED driver power consumption, is the goal of the work presented in this paper.

8.3 Compressive Sampling (CS) for Photoplethysmography (PPG) Acquisition and Feature Extraction from Compressively Sampled Signal

8.3.1 Compressive Sampling (CS) for Photoplethysmography (PPG) Acquisition

Compressive sampling (CS) is an alternate signal acquisition paradigm which asserts that certain class of signals can be faithfully recovered from far fewer samples or measurements of the signal compared to traditional Nyquist-based sampling [6]. This acquisition protocol relies on the *sparsity* of the signal on a given basis and its *incoherence* to the sampling scheme. Several physiological signals such as ECG, EEG, etc. have been shown to be sparse on standard bases such as the wavelet basis and Gabor basis. PPG signals, in particular, have been shown to be sparse on frequency basis [7]. Since the frequency basis is maximally incoherent to canonical basis, CS for PPG signals is equivalent to randomly subsampling the signal in time domain. In mathematical terms, the signal acquisition protocol in CS framework can be expressed as

$$Y = \Phi X \tag{8.1}$$

where Φ is referred to as the measurement matrix and Y and X are the M-dimensional measurement vector and the N-dimensional signal vector, respectively ($M \ll N$).

As indicated in (8.1), CS-based acquisition of a signal acquires a *linearly transformed, lower-dimensional* representation of the signal, often referred to as *measurements* rather than the actual signal. This approach, therefore, results in *compression* (and hence the name compressive sampling), which is usually quantified through the metric, compression ratio (CR) defined as

$$CR = \frac{N}{M} \tag{8.2}$$

The equivalent (partial) measurement matrix for random subsampling is shown in Fig. 8.3, which is $M \times N$ reduced order identity matrix, formed by choosing M rows from the $N \times N$ identity matrix at random. The M rows chosen at random correspond to the M sampling instants in time domain (with the row index corresponding to the sample index). In practice, pseudorandom subsampling schemes are used, showing

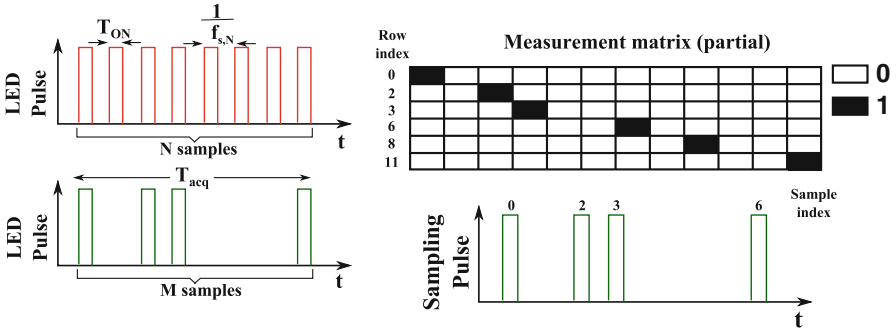

Fig. 8.3 Sampling sequence for CS PPG acquisition system and its equivalent measurement matrix structure

on par performance with fully random samples. The same pseudorandom sequence can be reused for every discrete window of length T_{acq} s (Fig. 8.3). Compared to the conventional PPG acquisition, based on uniform sampling, CS-based PPG acquisition acquires signal at an average sampling rate of $f_{s,CS}$ given by

$$f_{s,CS} = \frac{f_{s,N}}{CR}. \tag{8.3}$$

where $f_{s,N}$ is the uniform sampling rate.

Therefore, CS-based PPG acquisition systems have a LED driver duty cycle of $T_{ON} \times f_{s,CS}$ compared to $T_{ON} \times f_{s,N}$, as is the case for conventional uniform sampling PPG acquisition systems which hence enables reduction of LED driver power consumption by a factor of CR.

8.3.2 *Feature Extraction from Compressively Sampled (CS) Photoplethysmographic (PPG) Signal*

While the acquisition of a signal in the CS framework is relatively simple, recovering the signal back from the measurements, often referred to as the reconstruction process, is a very computationally intensive task. While several algorithms exist for signal recovery, with varying degrees of computational complexity [8], only a handful hardware implementations for the same exist [9–11]. Many CS implementations reported in the literature assume the presence of a powerful base station, to which the measurement data is off-loaded over a wireless link. The reconstruction is then performed at the base station, where the power constraints are relaxed (Fig. 8.4a). The advocates of this model [8, 12] argue that wireless transmission tends to dominate the sensor node power consumption in wireless sensor network (WSN) and body area network (BAN) applications, and hence transmitting the

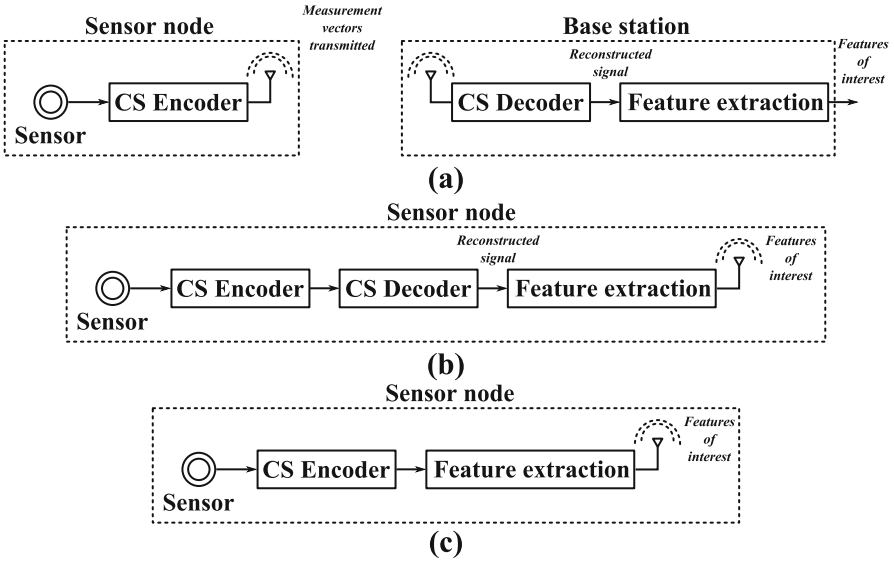

Fig. 8.4 Various possible CS-based acquisition systems in context of BAN. (**a**) Signal acquisition is performed at the sensor node, while reconstruction and feature extraction are performed at the base station. (**b**) Both CS encoding and decoding are performed on the signal node followed by feature extraction. (**c**) Feature extraction is performed on the sensor node directly from the CS data

compressed data rather than performing the reconstruction on the sensor node and then transmitting the data is efficient in terms of power consumption. This approach, therefore, shifts the problem of signal analysis and extracting the parameters of clinical interest to the base station. However, the need for analyzing the signal and extracting the relevant *features* locally on the sensor node is becoming important, particularly for privacy-and latency-sensitive biomedical applications [13]. Yet, locally reconstructing the signal on the sensor node (Fig. 8.4b) would consume power in the range of mWs [9], rendering feature extraction from the reconstructed signal on the sensor node infeasible for low-power sensing applications.[1]

Alternatively, the requirement of reconstructing the signal can be circumvented if the features of interest can be extracted directly from the CS data (Fig. 8.4c). This approach enables rapid signal analysis on energy-scarce BAN/WSN platforms directly from the CS data, without requiring complex reconstruction process. In this work, the use of least-squares spectral fitting techniques is explored for power

[1]The benefits of CS encoding and decoding, followed by feature extraction, all on the sensor node, over the conventional approach of performing feature extraction on the Nyquist rate sampled signal might not be obvious. CS-based approach can be useful in cases where high-power stimulation is involved, as in the case with PPG acquisition as well as in the cases where the maximum achievable sampling frequency of the ADC is limited [15].

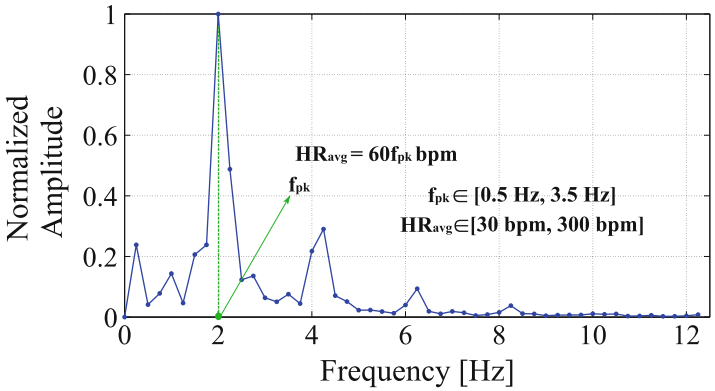

Fig. 8.5 Estimation of average HR from the frequency spectrum of PPG signal

spectral density (PSD) estimation directly from CS PPG signals. In particular, Lomb-Scargle periodogram (LSP) is used as the PSD estimator for randomly subsampled PPG signal [14]. Once the PSD is estimated, the average HR over time interval of T_{acq} can be estimated in the frequency domain by extracting the frequency corresponding to the peak in the PSD, f_{pk} as

$$HR_{\text{avg}} = 60 \cdot f_{pk}. \tag{8.4}$$

where HR_{avg} is the average HR in beats per minute (bpm) (Fig. 8.5). Once the average HR is estimated, HRV can be readily inferred from the variation of average HR across successive time intervals over which the spectrum is estimated.

The implementation details of a single-channel PPG readout ASIC [16], leveraging on the concepts of CS and feature extraction from CS domain discussed in this section, are presented in Sect. 8.4.

8.4 Compressive Sampling (CS) Photoplethysmographic (PPG) Readout Implementation

8.4.1 ASIC Implementation

The top-level architecture of the single-channel CS PPG acquisition ASIC is shown in Fig. 8.6. The ASIC embeds an AFE which performs a pseudorandom subsampled acquisition of the PPG signal and a digital back-end (DBE), which performs the HR estimation directly from the CS PPG signal. The AFE integrates a programmable gain TIA, the output of which is interfaced to a switched integrator (SI), which improves the SNR. The output of the SI is buffered and digitized through a 12-bit SAR ADC. A sub-1V bandgap reference is integrated on-chip to provide stable

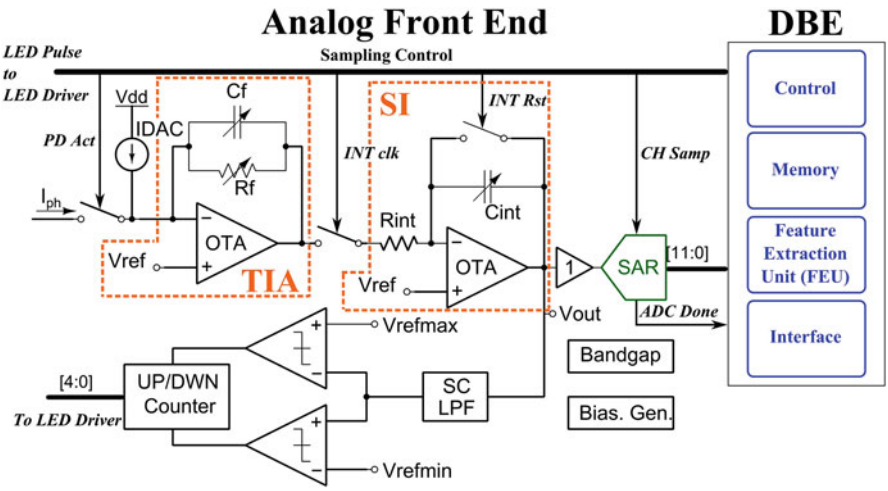

Fig. 8.6 The architecture of a single-channel CS PPG acquisition ASIC which embeds a DBE for feature extraction

on-chip bias and reference signals. The DBE comprises of a control unit (CU) that generates the necessary control signals required for the LED driver, AFE, and the ADC and also the required internal timing and synchronizing signals. Direct memory access (DMA) is integrated into the DBE which transfers the incoming data from the ADC into one of the data memory (DMEM) banks. The feature extraction unit (FEU), also part of the DBE, accelerates the process of LSP to enable extraction of HR directly from the CS PPG signal. The DBE is clocked through an external clock at 32 kHz. The ASIC also provides wide-scale programmability both for the gain and bandwidth settings of the AFE and CR, thereby extending its utility across a wide range of photocurrent amplitudes.

The first stage of the readout channel is a TIA that is interfaced to an off-chip photodiode (PD). The TIA converts the PPG signal that is acquired as a current signal at the output of the PD into a voltage signal, which is further processed by the signal processing chain in voltage domain. The TIA is realized by employing resistive feedback (R_f) around a two-stage Miller-compensated OTA. The large reverse bias junction capacitance of the PD, which manifests itself as a parasitic capacitance (C_p) at the inverting node, poses issues to the stability of the TIA. Hence, a compensation capacitor (C_f) is added in parallel to R_f to improve the stability margin of the TIA. As mentioned in Sect. 8.1, the relative large DC component of photocurrent necessitates the need for large DR for the readout. The channel DR requirements can however be relaxed if the DC component of the current is rejected early in the signal processing chain. This is achieved by interfacing a 5-bit current DAC (IDAC), capable of sourcing up to 10 μA of current at the input of the TIA.

The output of the TIA is fed into a switched integrator (SI), which is realized by incorporating a switched-capacitor (SC) in feedback around the OTA. The output of the TIA is converted into a current signal through R_{int}, which is then integrated onto C_{int} for a duration of T_{int}, thereby providing additional voltage amplification. The SI stage, apart from providing additional gain, also acts as a noise-limiting filter [17]. This is particularly important in pulsed PPG acquisition systems, where the thermal noise originating from the OTA of the TIA exhibits noise peaking at high frequencies. A mixed-signal feedback loop, comprised of a SC low-pass filter (SC LPF), comparators, and an up-down counter, tracks the output DC level of the SI. A 5-bit control code, to control the LED drive/IDAC current, is generated by the feedback loop such that the DC output of the SI stays within the threshold values (V_{refmin} and V_{refmax}), to ensure the proper utilization of the available channel DR.

The output of the SI is then digitized using a 12-bit SAR ADC, which comprises of a split capacitor DAC to reduce the area requirements, with a unit capacitance (C_u) of 800 fF. The pseudorandom subsampling instants of the ADC are controlled by the CU that forms part of the DBE. The digitized data, at the output of the ADC, is fed into the DBE for further processing to extract the HR. Interested readers are referred to [18], where the detailed description of the DBE architecture and implementation is presented.

8.4.2 Measurement Results

The ASIC is fabricated in a 0.18 μm process and occupies an area of 10 mm^2. To validate the functionality of the ASIC, an off-chip LED is modulated by a sinusoidal current with a frequency of 1.2 Hz (corresponding to 72 bpm HR), and the resulting PD current is read out for CRs of 8x and 30x as a voltage signal at the output of SI. As can been seen in Fig. 8.7, the acquired photocurrent and hence the voltage at the output of SI are (pseudo)random in nature and demonstrate the functionality of the AFE in CS acquisition mode. Figure 8.7 also shows an in vivo PPG acquisition, performed at 10x compression.

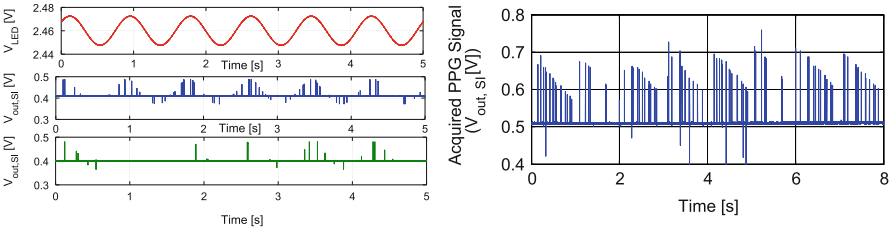

Fig. 8.7 (*Left*) Signal acquisition with CRs 8x and 30x when LED is stimulated with a sinusoidal current at 1.2 Hz. (*Right*) In vivo acquired PPG signal through the ASIC with a CR of 10x

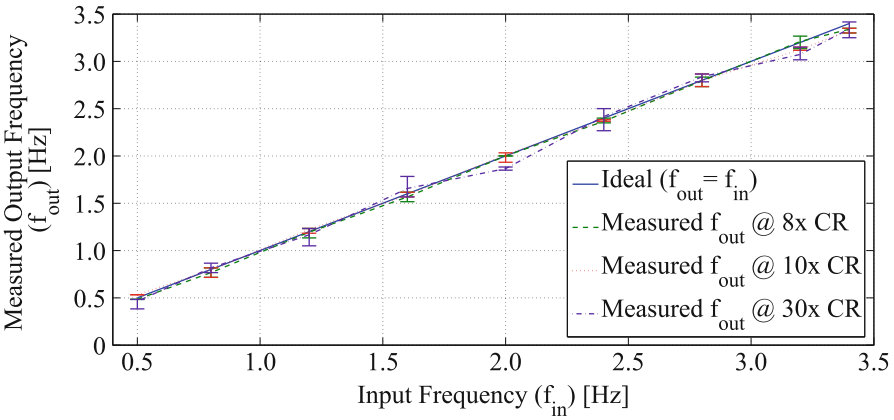

Fig. 8.8 Measured frequency corresponding to the peak in the PSD (f_{pk}) from the ASIC with LED modulated with a sinusoidal current whose frequency is swept from 0.5 to 3.4 Hz

The HR estimation performance is characterized by modulating the LED with a sinusoidal current, the frequency of which is swept from 0.5 to 3.4 Hz to cover the HR range of 30–204 bpm.[2] The LED modulation is carefully chosen so that the AC component of the photocurrent is approximately 20 nA_{pp}, which is comparable to the range of photocurrent measured while performing in vivo acquisition. The output of the readout is then compressively sampled with CRs 8x, 10x, and 30x, and feature extraction is performed on the acquired data. Since the feature extraction process estimates the frequency corresponding to the peak in the PSD, under ideal conditions, the estimated peak frequency (f_{pk}) should be identical to the input frequency. Figure 8.8 shows the extracted peak frequency for different CRs. The peak frequency serves as a proxy to estimate the HR using (8.4). The measured HR exhibits a worst-case error of 10 bpm at 30x compression for a nominal HR of 96 bpm. This error is still within the conformance specification provided by the ANSI-AAMI standards for heart rate meters [20].

Figure 8.9 shows the chip micrograph and the power consumption at different CRs. The ASIC consumes a total power of 172 μW from a supply of 1.2 V for the entire system of which the AFE consumes 158.8 μW, while the ADC and the DBE consume 6 μW and 7.2 μW, respectively. On the other hand, the LED driver power consumption scales from 1200 μW to 43 μW,[3] when scaling between uniform sampling mode (1x CR) and 30x CR, respectively, thanks to the compressive sampled acquisition paradigm. At lower CRs, LED driver continues to dominate the power consumption of the system, while at higher CRs, the AFE limits the power consumption due to fundamental noise limitations.

[2]Standard database [19] PPG signals lack annotations and hence sinusoidal modulation is chosen.

[3]The LED driver power consumption is measured while acquiring the PPG signal of a healthy individual. At the reported power levels, the resulting photocurrent is measured to have an AC component of 45 nA_{pp}, while the DC component is measured to be 1.6 μA.

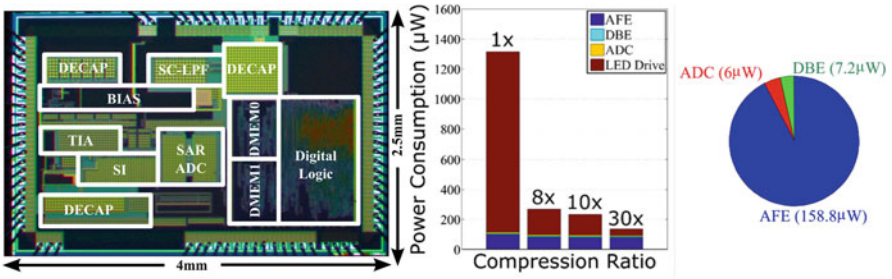

Fig. 8.9 The ASIC chip micrograph and measured power consumption breakdown of the ASIC and the off-chip LED driver for different CRs

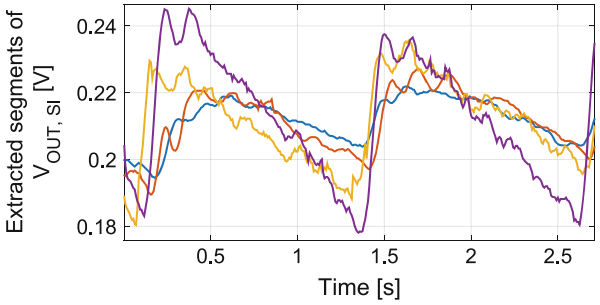

Fig. 8.10 In vivo acquired PPG signals under different SNR conditions. The corresponding values of acquired photocurrent and LED driver current are indicated in Table 8.1

Table 8.1 ASIC performance with different SNRs

AC component of PPG signal (Vpp)	**15 mV**	**25 mV**	**40 mV**	**60 mV**
AC component of photocurrent (I_{ac}(pp))	**3 nA**	**5 nA**	**8 nA**	**12 nA**
LED peak current	18 mA	56 mA	160 mA	314 mA
IDAC	312.5 nA	937.5 nA	2.1875 μA	2.5 μA
HR est.@CR = 10x	49	46	47	48
HR est.@CR = 1x(uni.)	48	48	48	48

The robustness of the ASIC under varying SNR conditions is demonstrated by performing in vivo acquisition of PPG under four different conditions, changing the LED driver current (drawn from a 5 V supply) while adjusting the IDAC setting to cancel most of the DC component out. The excerpts of the recorded PPG signals after being filtered are shown in Fig. 8.10. Table 8.1 shows the information of the different setups, the resulting AC component of the acquired signals, and the heart rate value calculated by the ASIC at a CR of 10x as well as with uniform sampling. The AC component of the photocurrent varies from 3 nA_{pp} for a LED driver peak current of 18 mA to 12 nA_{pp} when the LED driver peak current is increased to

314 mA. The HR, estimated from the uniformly sampled PPG signal using FFT, serves as the reference. The PPG signal is then compressively acquired at a CR of 10x, and the average HR estimated by the ASIC is compared against the reference. As can be seen in Table 8.1, the error in the average HR is estimated at 10x CR within 2 bpm under varying SNR conditions. The LED driver power consumption, on the other hand, scales proportional to the CR, from 6.1 mW to 615 μW for an acquired AC component of photocurrent of 12 nA_{pp}.

Finally, the performance of the CS PPG ASIC is summarized and compared against the state-of-the-art PPG acquisition systems in Table 8.2. Compared to the state-of-the-art, CS-based PPG, acquisition enables up to 30x reduction in the power consumption of the LED driver, thanks to the DBE, which accelerates LSP to enable feature extraction directly from CS data to accurately estimate HR with minimum power penalty.

8.5 Artifact Reduction and Electrocardiogram (ECG)-Assisted Photoplethysmogram (PPG) Acquisition

8.5.1 Artifact Reduction Through Spectral Subtraction

A wearable PPG acquisition system is usually subject to large amounts of motion. Depending on the location of the sensor and the nature of the motion, the artifacts in signals can manifest themselves in different ways, making it hard to derive HR and HRV from them. Unlike ECG, motion can potentially alter the flow of blood in the tissue, affecting the physiological signal in a rather fundamental way. An immediate consequence of large motion artifacts is the need for large DR for the PPG readout. Yet, even for PPG readouts with large DR, processing the signal infested with artifacts to extract relevant features such as HR is extremely challenging.

An attempt to mitigate motion artifacts in PPG acquisition systems was made by [4]. The authors in [4] rely on mechanically stabilizing the LED and PD pair housed in a double-ringed aluminum unit. This mechanical approach, however, is limited to PPG sensors that have a specific form factor – the ones that can be worn as a ring.

Figure 8.11 shows an alternate approach to mitigate motion artifacts in the digital domain. This process involves spectral estimation of PPG signals using the LSP approach. Simultaneously, a representative motion signal, such as the output of an accelerometer, is pseudorandomly subsampled, with the same sampling sequence as used for the PPG aignal. Subsequently, spectral estimation is performed using the LSP. The output spectra are then normalized and subtracted from each other to remove the motion component. Since this approach involves *denoising* through subtraction in the frequency domain, it is referred to as *spectral subtraction* technique and is popularly used to eliminate the background noise in speech signal processing [24].

Table 8.2 ASIC performance summary and comparison with the state-of-the-art

	This work	TBCAS'10 [21]	ISSCC'13 [5]	TBCAS'08 [22]	TBCAS'15 [23]
Tech. & supply	**0.18 μm CMOS 1.2 V**	1.5 μm BiCMOS 5 V	0.18 μm CMOS 0.5 V	0.35 μm CMOS 2.5 V	0.18 μm CMOS 1.8 V
Sampling frequency	**128, 16, 13 and 4 Hz**[a]	100 Hz	32 kHz	100 Hz	165 Hz
DC current cancelation	**Up to 10 μA**	NR	Up to 4 μA	53.6 μA (Ext. HPF)	100 μA
Integrated noise (RTI)	**486 pA_{rms}**[b]	NR	NR	2.2 nA_{rms}	600 pA_{rms}
Noise bandwidth	**10 Hz**	NR	NR	6 Hz	10 Hz
Integrated feature extraction	**Yes (HR/HRV)**	Yes (SpO_2[c])	No	No	No
Data compression	**Yes (8x, 10x, 30x)**	No	No	No	No
Power consumption (Readout)	**172 μW**[d]	400 μW	4 μW	600 μW	216 μW
Power consumption (LED driver)	**1200–43 μW**[e]	4400 μW	NA (ambient light)	NR	1125–120 μW

NA Not applicable, *NR* Not reported
[a]Average sampling frequencies corresponding to CRs 8x, 10x and 30x respectively
[b]TIA setting: $R_f = 50\,k\Omega$ and $C_f = 6\,pF$
[c]Blood oxygenation saturation measurement
[d]Includes AFE, ADC, DBE (while executing feature extraction) and bias power consumption, with power down mode disabled
[e]Off-chip LED driver. LED power consumption is subject to the SNR, skin tone of the subject and the efficiency of the LED used in the setup

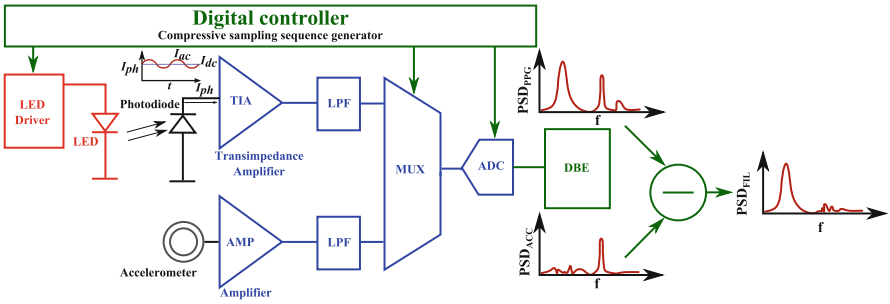

Fig. 8.11 Concept of motion artifact reduction using spectral subtraction

To demonstrate the efficacy of the proposed technique, PPG signals (Fig. 8.12a) are acquired using an internal PPG acquisition platform built from commercial off-the-shelf (COTS) components, from a subject under normal office working conditions. Simultaneously, accelerometer signals (Fig. 8.12c) are acquired using the same platform. The PPG and accelerometer signals are then randomly subsampled by a CR of 10x, and LSP is performed on both subsampled signals in MATLAB[6]. Spectral subtraction is finally performed on the normalized LSP of PPG and accelerometer signal and is rescaled. The rescaling process uses a scale factor that renormalizes the PSD of the *spectral subtracted* PPG signal, thereby restoring the amplitude of the peak in the PSD of the PPG signal. Figure 8.12e shows the spectral subtracted PSD of the PPG signal, and as can be seen, the spurious peak in the frequency range [2.7–3.2 Hz] that is correlated to the motion is significantly suppressed by spectral subtraction.

It must however be noted that while simulation results on a limited data set show promising results, extensive characterization of the technique is required under a variety of use case scenarios to arrive at a concrete conclusion regarding its efficacy under different motion artifact scenarios. Moreover, this technique is only a post-processing step and does not mitigate the requirement of a high channel DR. While an adaptive filter-based approach, presented in [25] for ECG, is promising to relax the DR requirements, it is challenging to design adaptive filters that work with randomly subsampled data.

8.5.2 Electrocardiogram (ECG)-Assisted Photoplethysmogram (PPG) Acquisition

Cuffless blood pressure (BP) monitoring using combination of ECG and PPG has been demonstrated in [23, 26]. The determination of BP is based on the relative timing between peaks in the ECG and PPG signals. Figure 8.13 shows the relevant timing information required for the BP estimation. Of interest is the pulse arrival time (PAT), which is the temporal difference between the peak in the ECG and

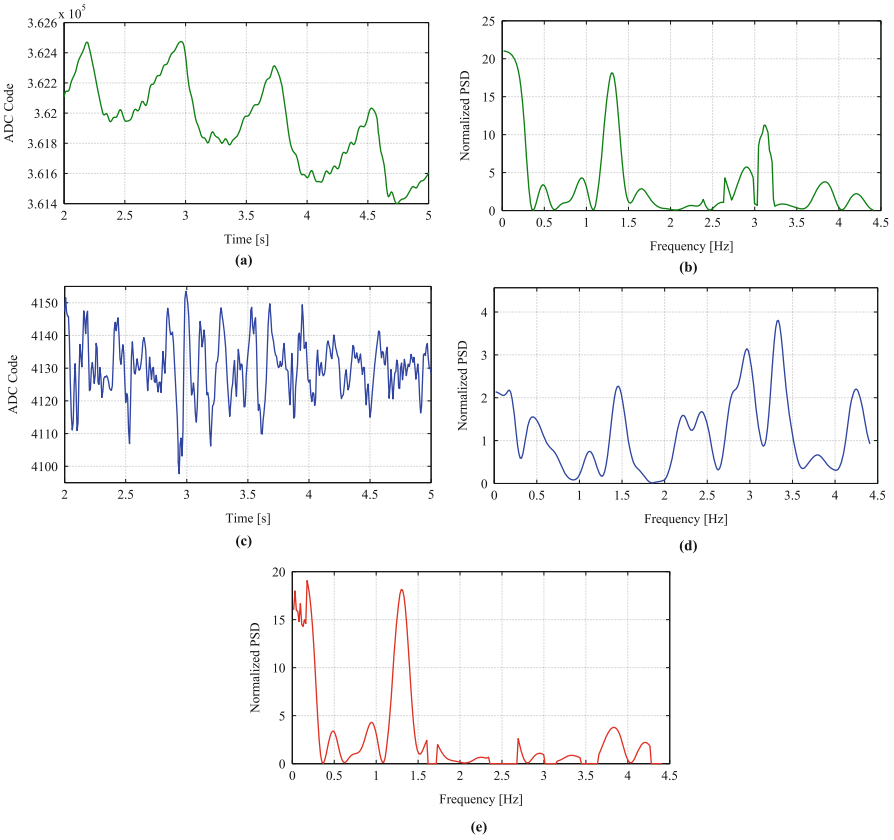

Fig. 8.12 (**a**) PPG signal acquired from a subject under normal office working conditions. (**b**) PSD of the PPG signal estimated using LSP after 10x random subsampling. (**c**) Accelerometer signal acquired simultaneous to PPG acquisition. (**d**) PSD of the accelerometer signal estimated using LSP after 10x random subsampling. (**e**) PSD of the PPG signal post spectral subtraction

the subsequent peak in the PPG signal. Once PAT is determined, BP is estimated using (8.5).

$$\begin{aligned} SBP &= a_1 \cdot PAT + b_1 \cdot HR + c_1 \\ DBP &= a_2 \cdot PAT + b_2 \cdot HR + c_2 \end{aligned} \tag{8.5}$$

where *SBP* and *DBP* are the systolic and diastolic blood pressure, respectively, while a_i, b_i and c_i, for $i = 1, 2$ are the calibration coefficients obtained through linear regression.

While the implementations in [23, 26] report achieving sufficient accuracy in determining BP for wearable applications, their power consumption is dominated by the PPG system, owing to the uniform stimulation and sampling. [12] demonstrated

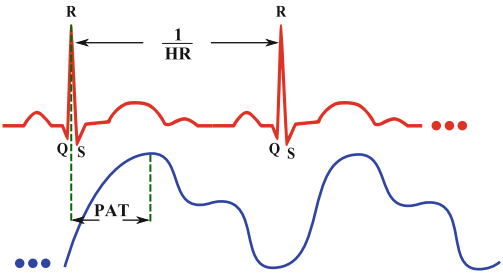

Fig. 8.13 Determination of PAT and HR for cuffless BP estimation

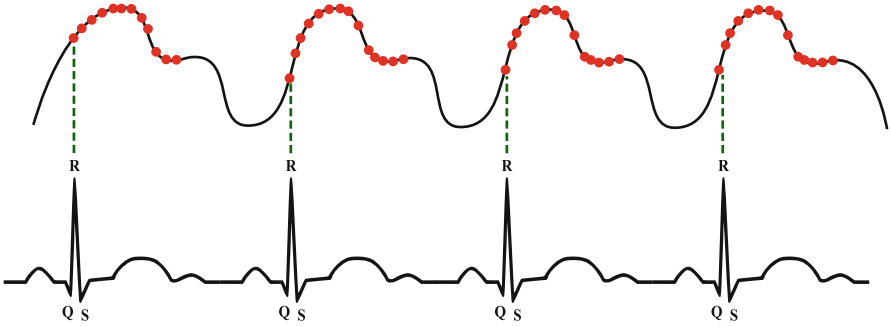

Fig. 8.14 ECG-assisted PPG acquisition for cuffless BP estimation

the use of CS-based PPG for cuffless BP estimation. However, [12] employs a full signal reconstruction process to perform BP determination from the reconstructed PPG signal, with the assumption of the availability of a powerful base station. As discussed in Sect. 8.3.2, the overhead in the reconstruction process can potentially cancel all power savings obtained from CS acquisition of PPG.

Alternatively, an event-driven approach that relies on the *assistance* from ECG to acquire PPG can be explored. Realizing that the peak in PPG signal is the aftereffect of the pumping action of blood through vessels by the heart, one can utilize the occurrence of the QRS complex to trigger the capture of the PPG signal. The acquisition can be stopped, when sufficient number of samples are acquired around the peak of the PPG signal. This approach is shown in Fig. 8.14. The presence of QRS complexes in the ECG can easily be detected using the activity detection process outlined in [27]. While a wide range of stopping criteria can be used for the PPG sampling, ranging from simple thresholding to more complex approaches based on learning, in this work a sum of slopes followed by thresholding is employed. Figure 8.15 shows a 10 s simultaneous ECG and PPG recording obtained through the COTS platform. The PPG signal is then adaptively resampled in ECG-*assisted* sampling mode, with the ECG signal acting as the trigger for PPG acquisition. For the recordings shown in Fig. 8.15, only 446 samples of PPG signal are acquired in the ECG-*assisted* acquisition mode as against 1280 in the uniform sampling mode, leading to an average stimulation and sampling frequency reduction

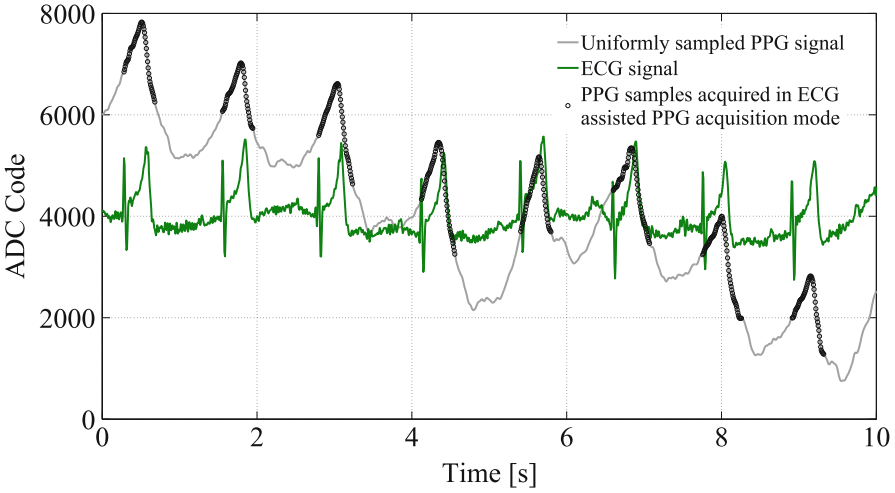

Fig. 8.15 A 10 s simultaneous ECG and PPG recording obtained through the COTS platform (average values are equalized for better representation). Both signals are sampled at 128 Hz

by a factor of 2.9. Since the relative timing information of interest is completely preserved in the ECG-*assisted* acquisition mode, both SBP and DBP are estimated with the same degree of accuracy as in the case of uniform sampling mode. It must however be noted that the amount of stimulation and sampling rate reduction depends on several factors including the relative placement of the ECG and the PPG sensors. To further validate this approach, MATLAB[6] simulations are run for ten different records, also obtained using the COTS platform. Simulation results demonstrate the possibility of reduction of the average stimulation and sampling frequency of PPG by a factor of 1.8 (averaged across the ten records). While this factor is small compared to the CS-based approach reported in [12], the proposed approach neither requires a base station nor involves a complex reconstruction process.

8.6 Conclusions

A compressive sampling (CS) photoplethysmographic (PPG) readout with embedded feature extraction is described. The feature extraction process exploits the Lomb-Scargle periodogram (LSP) to extract heart rate (HR) directly from CS PPG signal, thereby mitigating the need for complex reconstruction techniques. The implemented ASIC advances the state of the art by reducing the relative LED driver consumption by up to 30x while estimating the average HR with an accuracy conforming to the ANSI-AAMI standard for heart rate meters. The ASIC, implemented in a standard 0.18 μm CMOS process, consumes 172 μW

of power from a 1.2 V supply, with the digital back-end (DBE) consuming only 7.2 μW, thus avoiding the energy penalties of wireless/wire line transmission and/or embedded signal reconstruction. In addition, a digital domain motion artifact suppression technique leveraging on multisensor fusion is presented. The proposed technique leverages on the *spectral subtraction* of the power spectral density (PSD) estimated for PPG signals and accelerometer signals. The efficacy of the technique is demonstrated through simulations. Finally, an electrocardiogram (ECG)-assisted PPG acquisition system is described for cuffless blood pressure (BP) monitoring. The proposed approach retains the relevant relative timing information between the ECG and the PPG signals, yet facilitating accurate BP estimation at a reduced average stimulation and sampling rate by a factor of 1.8 across ten records obtained using a COTS platform.

References

1. Wijsman, J., Grundlehner, B., Liu, H., Hermens, H., Penders, J.: Towards mental stress detection using wearable physiological sensors. In: 2011 Annual International Conference of the IEEE Engineering in Medicine and Biology Society, pp. 1798–1801, Aug 2011
2. Allen, J.: Photoplethysmography and its application in clinical physiological measurement. Physiol. Meas. **28**(3), R1 (2007)
3. Webster, J.G.: Design of Pulse Oximeters. Taylor & Francis Group, New York (1997)
4. Rhee, S., Yang, B.-H., Asada, H.: Artifact-resistant power-efficient design of finger-ring plethysmographic sensors. IEEE Trans Biomed. Eng. **48**(7), 795–805 (2001)
5. Alhawari, M., Albelooshi, N., Perrott, M.H.: A 0.5 V $<$ 4 μW CMOS photoplethysmographic heart-rate sensor IC based on a non-uniform quantizer. In: 2013 IEEE International Solid-State Circuits Conference Digest of Technical Papers, pp. 384–385 (2013)
6. Candès, E.J., Wakin, M.B.: An introduction to compressive sampling. IEEE Signal Process. Mag. **25**(2), 21–30 (2008)
7. Pamula, V.R., Verhelst, M., Van Hoof, C., Yazicioglu, R.F.: Computationally-efficient compressive sampling for low-power pulse oximeter system. In: 2014 IEEE Biomedical Circuits and Systems Conference (BioCAS) Proceedings, pp. 69–72 (2014)
8. Dixon, A.M., Allstot, E.G., Gangopadhyay, D., Allstot, D.J.: Compressed sensing system considerations for ECG and EMG wireless biosensors. IEEE Trans. Biomed. Circuits Syst. **6**(2), 156–166 (2012)
9. Ren, F., Marković, D.: A configurable 12–237 kS/s 12.8 mW sparse-approximation engine for mobile data aggregation of compressively sampled physiological signals. IEEE J. Solid-State Circuits **51**(1) 68–78 (2016)
10. Maechler, P., Studer, C., Bellasi, D.E., Maleki, A., Burg, A., Felber, N., Kaeslin, H., Baraniuk, R.G.: VLSI design of approximate message passing for signal restoration and compressive sensing. IEEE J. Emerging Sel. Top. Circuits Syst. **2**(3), 579–590 (2012)
11. Maechler, P., Greisen, P., Sporrer, B., Steiner, S., Felber, N., Burg, A.: Implementation of greedy algorithms for LTE sparse channel estimation. In: 2010 Conference Record of the Forty Fourth Asilomar Conference on Signals, Systems and Computers, Nov 2010
12. Baheti, P.K., Garudadri, H.: An ultra low power pulse oximeter sensor based on compressed sensing. In: 2009 Sixth International Workshop on Wearable and Implantable Body Sensor Networks, Jun 2009
13. Csavoy, A., Molnar, G., Denison, T.: Creating support circuits for the nervous system: Considerations for brain-machine interfacing. In 2009 Symposium on VLSI Circuits, Jun 2009

14. Pamula, V.R., Verhelst, M., Van Hoof, C., Yazicioglu, R.F.: A novel feature extraction algorithm for on the sensor node processing of compressive sampled photoplethysmography signals. In: 2015 IEEE SENSORS, pp. 1–4. IEEE (2015)
15. Yoo, J., Turnes, C., Nakamura, E.B., Le, C.K., Becker, S., Sovero, E.A., Wakin, M.B., Grant, M.C., Romberg, J., Emami-Neyestanak, A., Candes, E.: A compressed sensing parameter extraction platform for radar pulse signal acquisition. IEEE IEEE J. Emerging Sel. Top. Circuits Syst. **2**(3), 626–638 (2012)
16. Rajesh, P.V., Valero-Sarmiento, J.M., Yan, L., Bozkurt, A., Van Hoof, C., Van Helleputte, N., Yazicioglu, R.F., Verhelst, M.: A 172 μW compressive sampling photoplethysmographic readout with embedded direct heart-rate and variability extraction from compressively sampled data. In: 2016 IEEE International Solid-State Circuits Conference (ISSCC), pp. 386–387. IEEE, Piscataway (2016)
17. Glaros, K.N., Drakakis, E.M.: A sub-mW fully-integrated pulse oximeter front-end. IEEE Trans. Biomed. Circuits Syst. **7**(3), 363–375 (2013)
18. Pamula, V.R., Valero-Sarmiento, J.M., Yan, L., Bozkurt, A., Van Hoof, C., Van Helleputte, N., Yazicioglu, R.F., Verhelst, M.: A 172_W compressively sampled photoplethysmographic (PPG) readout ASIC with heart rate estimation directly from compressively sampled data. IEEE Trans. Biomed. Circuits Syst. **11**(3), 487–496 (2017). Available online at IEEE Xplore
19. Goldberger, A.L., Amaral, L.A., Glass, L., Hausdorff, J.M., Ivanov, P.C., Mark, R.G., Mietus, J.E., Moody, G.B., Peng, C.-K., Stanley, H.E.: Physiobank, physiotoolkit, and physionet components of a new research resource for complex physiologic signals. Circulation **101**(23), 215–220 (2000)
20. ANSI/AAMI-EC13: American National Standards for cardiac monitors, hearth rate meters and alarms (2002)
21. Tavakoli, M., Turicchia, L., Sarpeshkar, R.: An ultra-low-power pulse oximeter implemented with an energy-efficient transimpedance amplifier. IEEE Trans. Biomed. Circuits Syst. **4**(1), 27–38 (2010)
22. Wong, A.K., Pun, K.-P., Zhang, Y.-T., Leung, K.N.: A low-power CMOS front-end for photoplethysmographic signal acquisition with robust DC photocurrent rejection. IEEE Trans. Biomed. Circuits Syst. **2**(4), 280–288 (2008)
23. Winokur, E.S., O'Dwyer, T., Sodini, C.G.: A low-power, dual-wavelength photoplethysmogram (PPG) SoC with static and time-varying interferer removal. IEEE Trans. Biomed. Circuits Syst. **9**(4), 581–589 (2015)
24. Boll, S.: Suppression of acoustic noise in speech using spectral subtraction. IEEE Trans. Acoust. Speech Signal Process. **27**(2), 113–120 (1979)
25. Helleputte, N.V., Kim, S., Kim, H., Kim, J.P., Hoof, C.V., Yazicioglu, R.F.: A 160 μA biopotential acquisition IC with fully integrated IA and motion artifact suppression. IEEE Trans. Biomed. Circuits Syst. **6**(6), 552–561 (2012)
26. Poon, C., Zhang, Y.: Cuff-less and noninvasive measurements of arterial blood pressure by pulse transit time. In: 2005 IEEE Engineering in Medicine and Biology 27th Annual Conference (2005)
27. Pamula, V.R., Verhelst, M., Hoof, C.V., Yazicioglu, R.F.: A 17 nA, 47.2 dB dynamic range, adaptive sampling controller for online data rate reduction in low power ECG systems. In: 2016 IEEE Biomedical Circuits and Systems Conference (BioCAS), pp. 272–275, Oct 2016